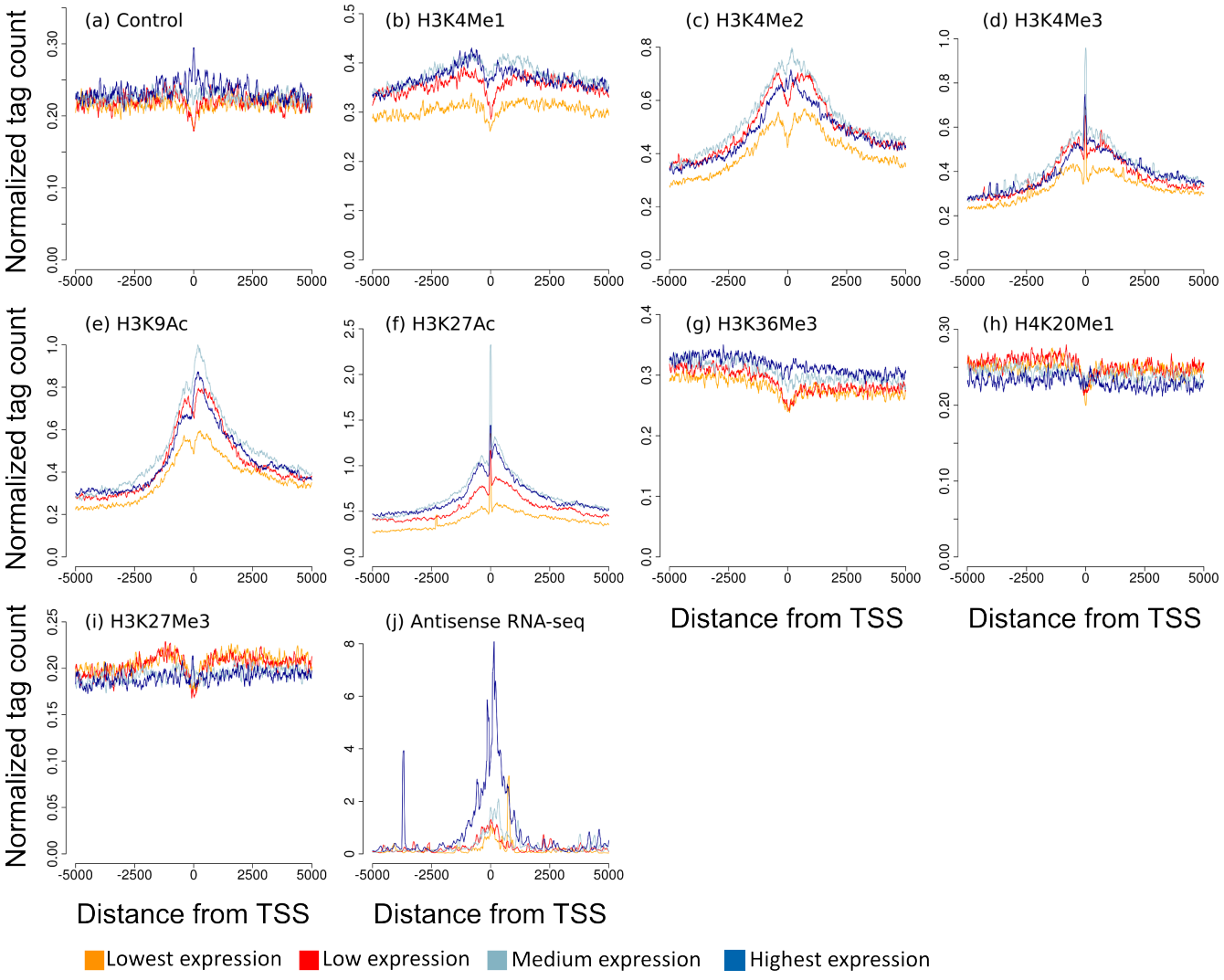

Supplementary Figure S32. Chromatin modification environment around cis-NAT promoters in GM12878. Cis-NAT promoters in the GM12878 cell type were identified using CAGE data from non-polyadenylated RNA from cytosol isolates. Cis-NAT promoters were divided into 4 bins based on their activity (lowest to highest), and the normalized average numbers of ChIP-seq reads in 10 base-pair windows +/- 5kb of the cis-NAT TSS (at position 0) were calculated for each bin.

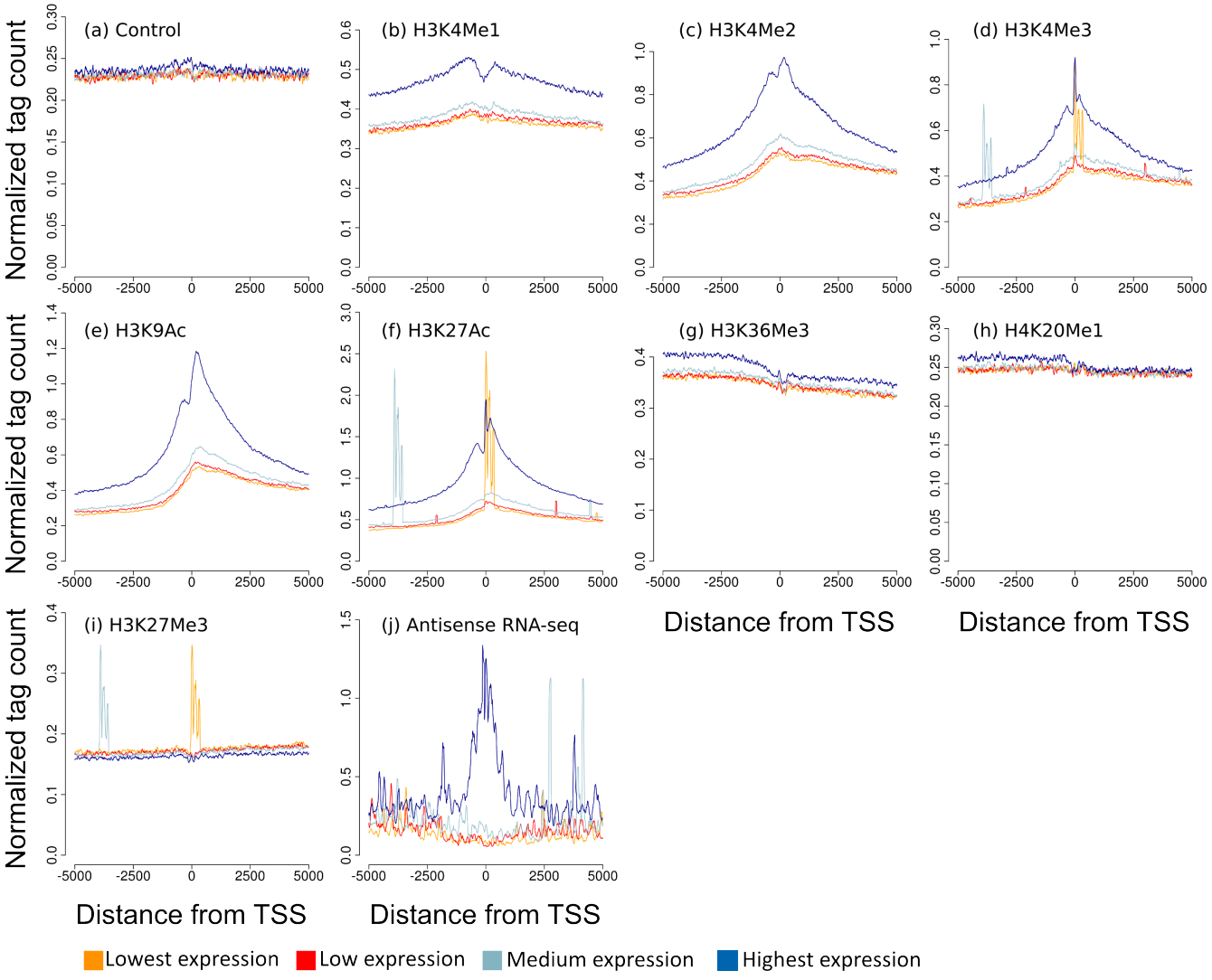

Supplementary Figure S33. Chromatin modification environment around cis-NAT promoters in GM12878. Cis-NAT promoters in the GM12878 cell type were identified using CAGE data from total RNA from nucleolus isolates. Cis-NAT promoters were divided into 4 bins based on their activity (lowest to highest), and the normalized average numbers of ChIP-seq reads in 10 base-pair windows +/- 5kb of the cis-NAT TSS (at position 0) were calculated for each bin.

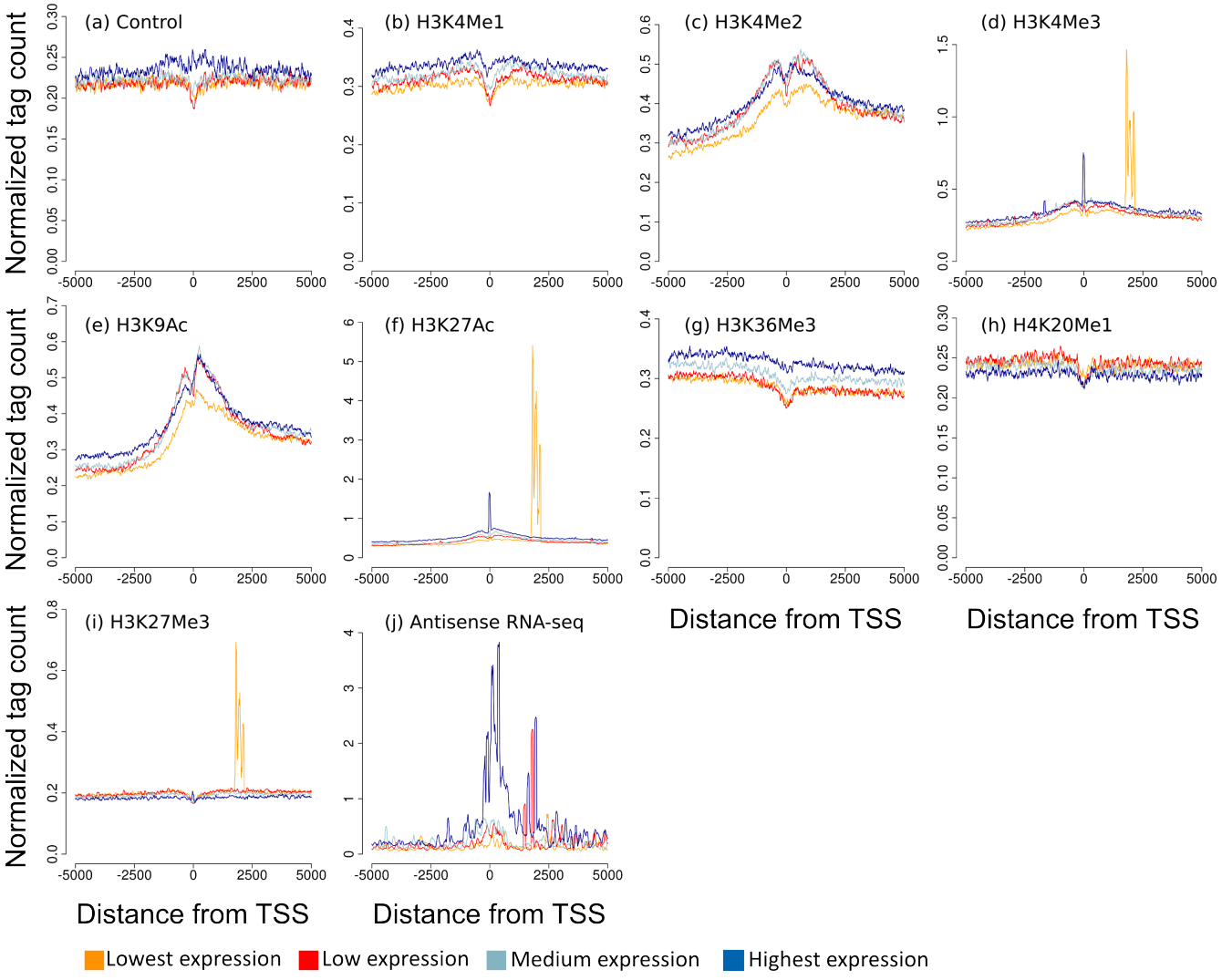

Supplementary Figure S34. Chromatin modification environment around cis-NAT promoters in GM12878. Cis-NAT promoters in the GM12878 cell type were identified using CAGE data from non-polyadenylated RNA from nucleus isolates. Cis-NAT promoters were divided into 4 bins based on their activity (lowest to highest), and the normalized average numbers of ChIP-seq reads in 10 base-pair windows +/- 5kb of the cis-NAT TSS (at position 0) were calculated for each bin.

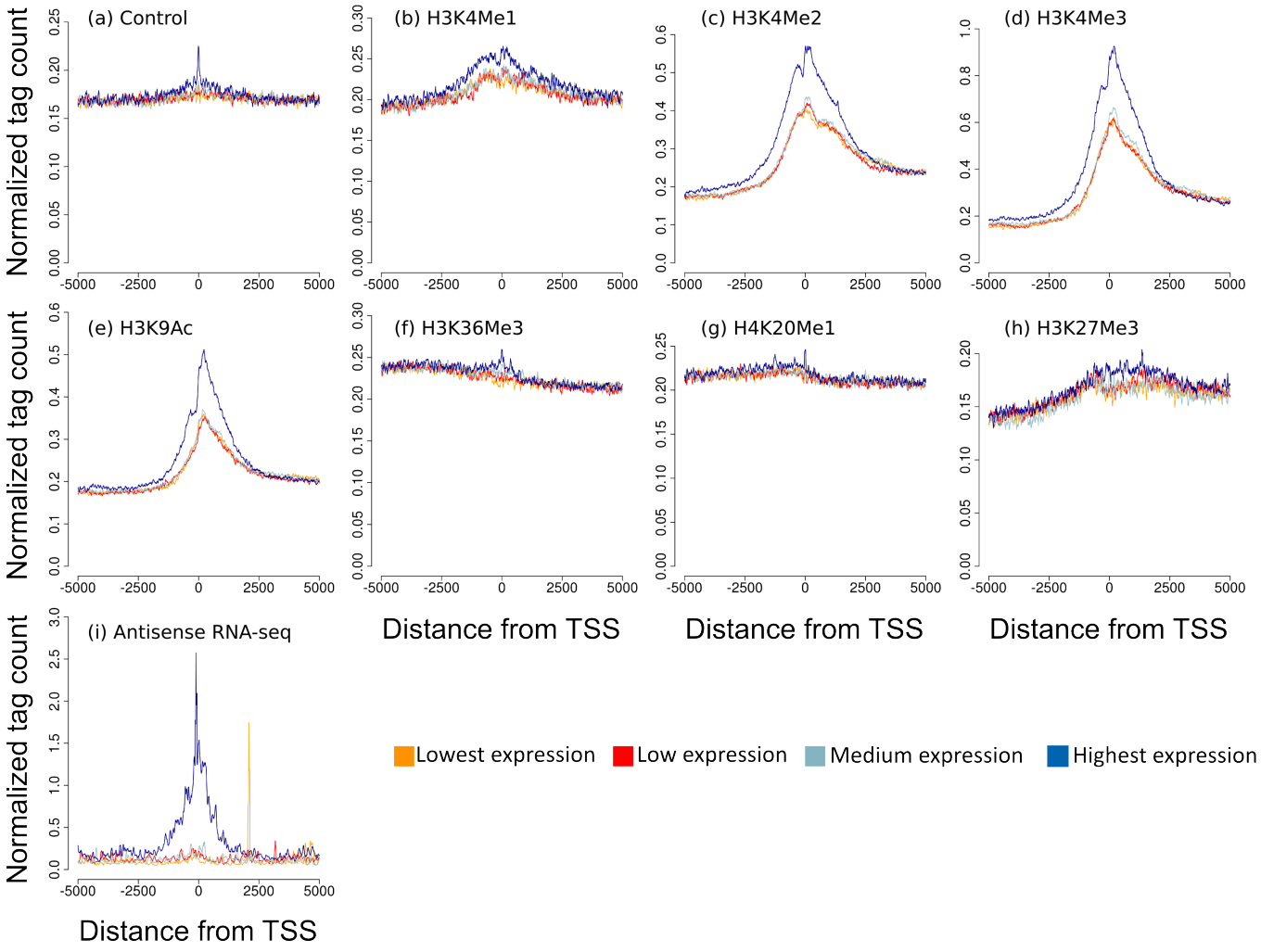

Supplementary Figure S35. Chromatin modification environment around cis-NAT promoters in H1HESC. Cis-NAT promoters in the H1HESC cell type were identified using CAGE data from non-polyadenylated RNA from whole-cell isolates. Cis-NAT promoters were divided into 4 bins based on their activity (lowest to highest), and the normalized average numbers of ChIP-seq reads in 10 base-pair windows +/- 5kb of the cis-NAT TSS (at position 0) were calculated for each bin.

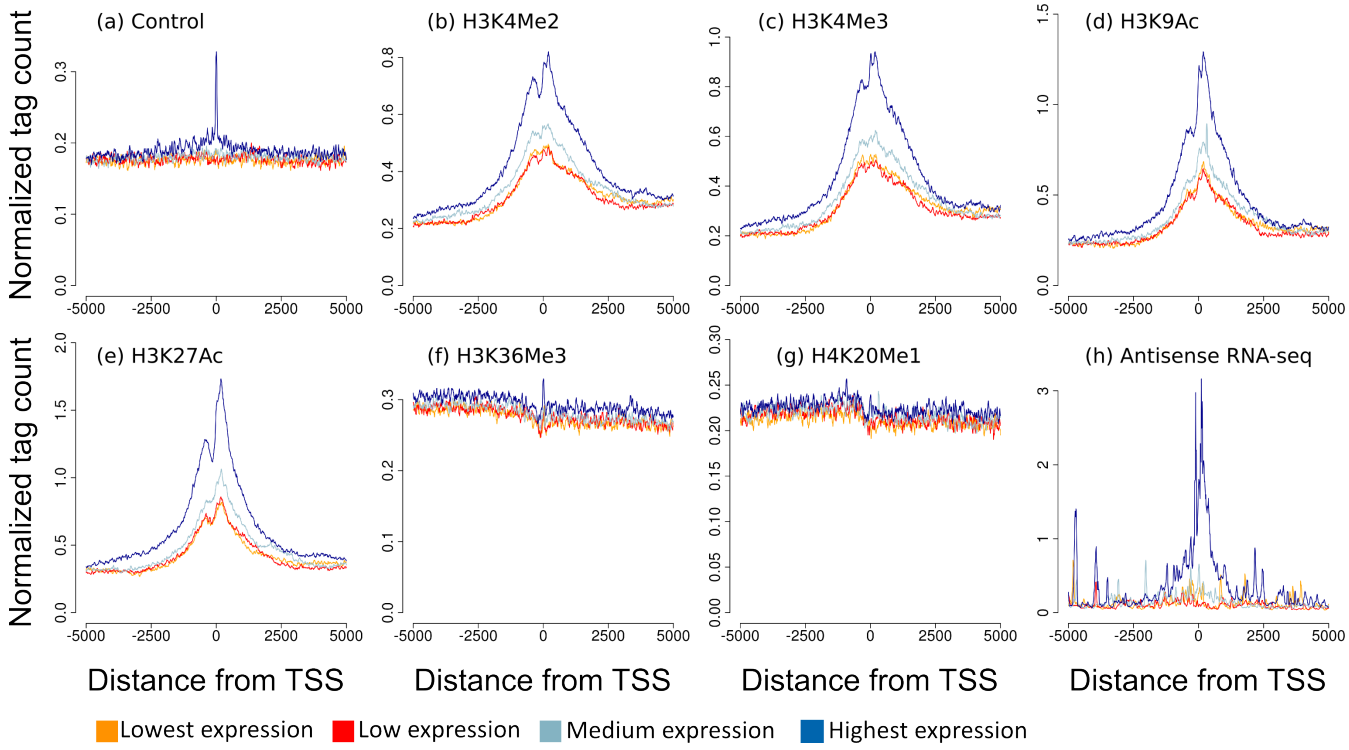

Supplementary Figure S36. Chromatin modification environment around cis-NAT promoters in HepG2. Cis-NAT promoters in the HepG2 cell type were identified using CAGE data from non-polyadenylated RNA from cytosol isolates. Cis-NAT promoters were divided into 4 bins based on their activity (lowest to highest), and the normalized average numbers of ChIP-seq reads in 10 base-pair windows +/- 5kb of the cis-NAT TSS (at position 0) were calculated for each bin.

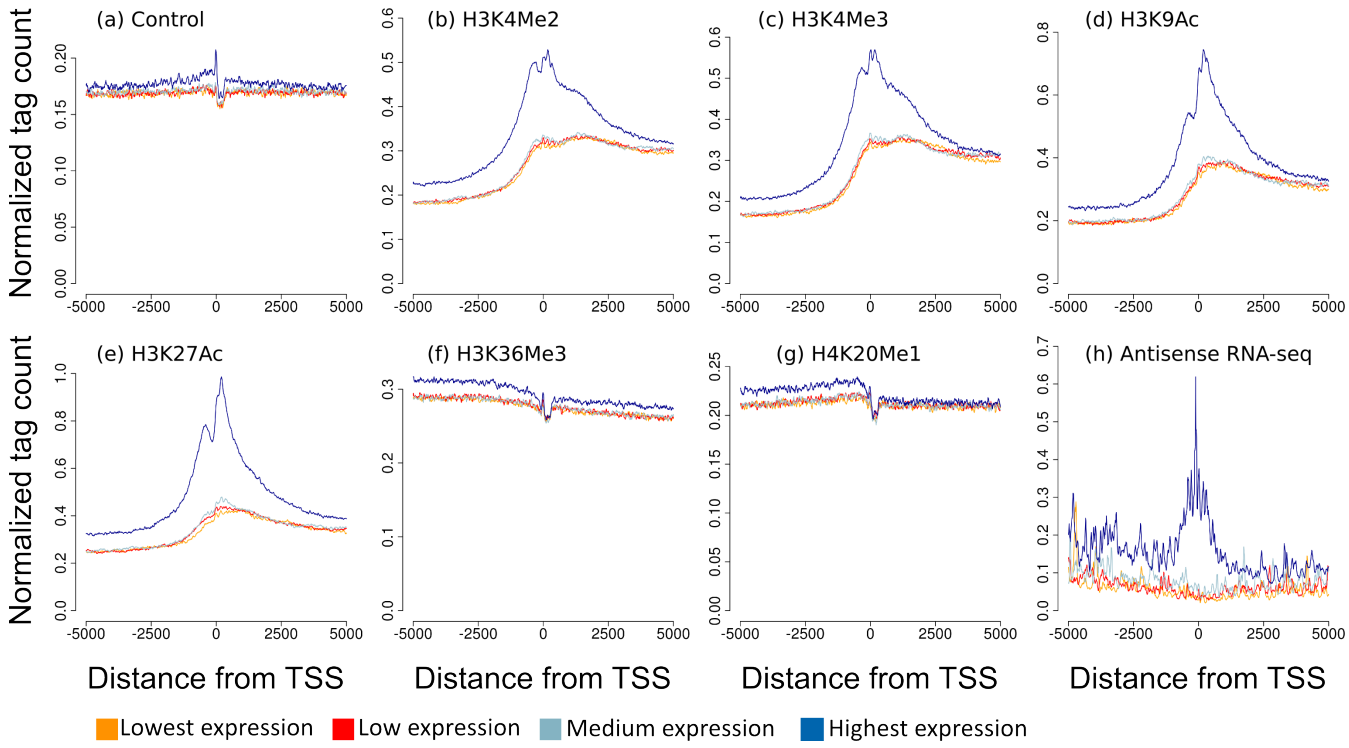

Supplementary Figure S37. Chromatin modification environment around cis-NAT promoters in HepG2. Cis-NAT promoters in the HepG2 cell type were identified using CAGE data from total RNA from nucleolus isolates. Cis-NAT promoters were divided into 4 bins based on their activity (lowest to highest), and the normalized average numbers of ChIP-seq reads in 10 base-pair windows +/- 5kb of the cis-NAT TSS (at position 0) were calculated for each bin.

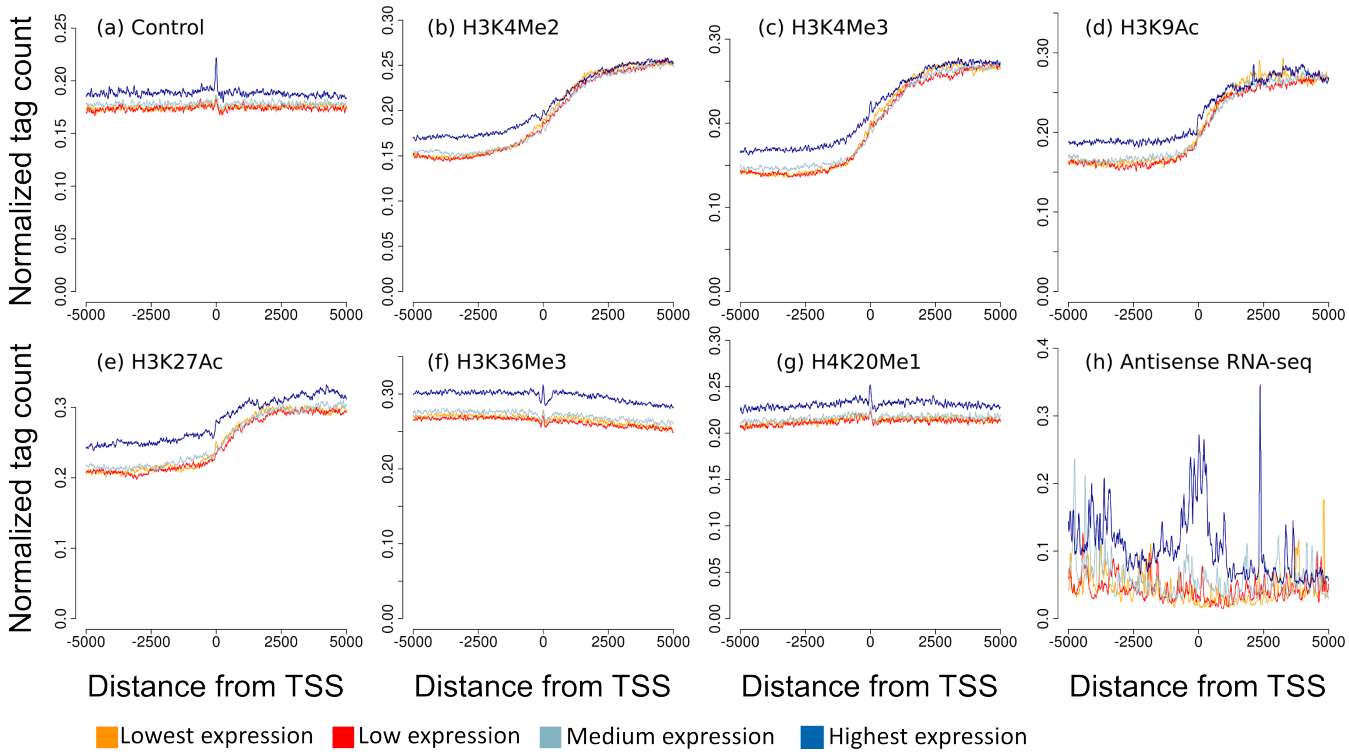

Supplementary Figure S38. Chromatin modification environment around cis-NAT promoters in HepG2. Cis-NAT promoters in the HepG2 cell type were identified using CAGE data from non-polyadenylated RNA from nucleus isolates. Cis-NAT promoters were divided into 4 bins based on their activity (lowest to highest), and the normalized average numbers of ChIP-seq reads in 10 base-pair windows +/- 5kb of the cis-NAT TSS (at position 0) were calculated for each bin.

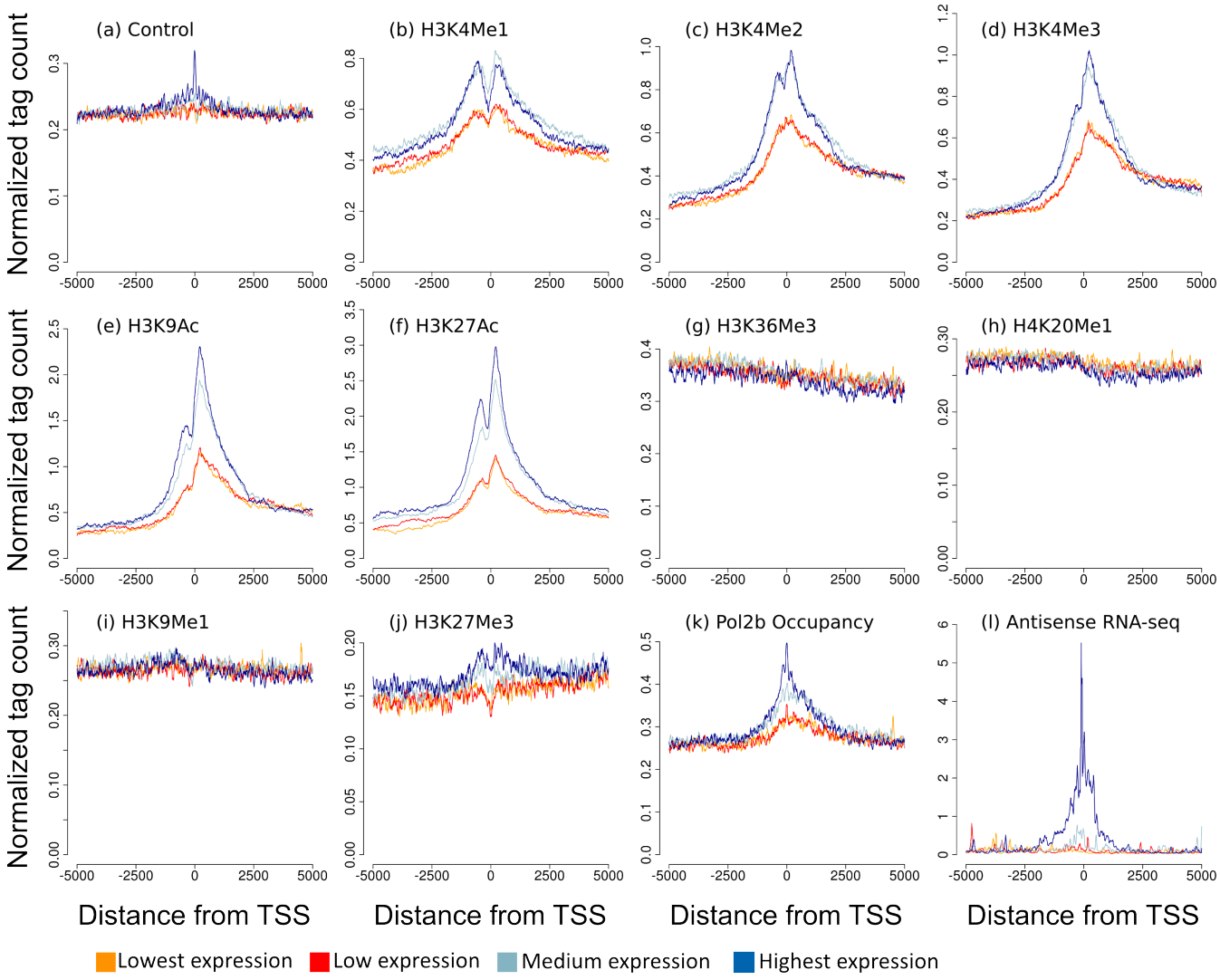

Supplementary Figure S39. Chromatin modification environment around cis-NAT promoters in HUVEC. Cis-NAT promoters in the HUVEC cell type were identified using CAGE data from non-polyadenylated RNA from cytosol isolates. Cis-NAT promoters were divided into 4 bins based on their activity (lowest to highest), and the normalized average numbers of ChIP-seq reads in 10 base-pair windows +/- 5kb of the cis-NAT TSS (at position 0) were calculated for each bin.

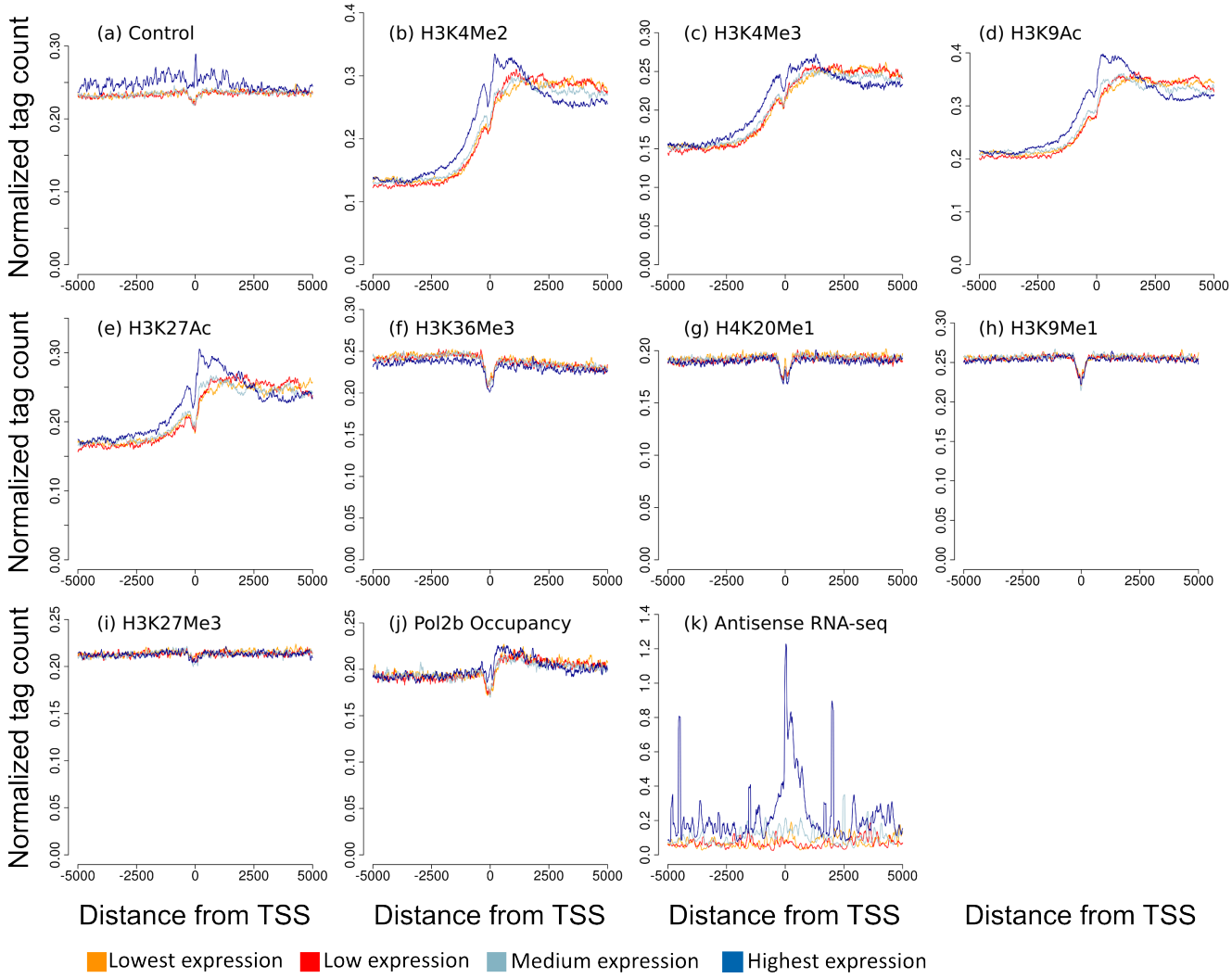

Supplementary Figure S40. Chromatin modification environment around cis-NAT promoters in K562. Cis-NAT promoters in the K562 cell type were identified using CAGE data from non-polyadenylated RNA from cytosol isolates. Cis-NAT promoters were divided into 4 bins based on their activity (lowest to highest), and the normalized average numbers of ChIP-seq reads in 10 base-pair windows +/- 5kb of the cis-NAT TSS (at position 0) were calculated for each bin.

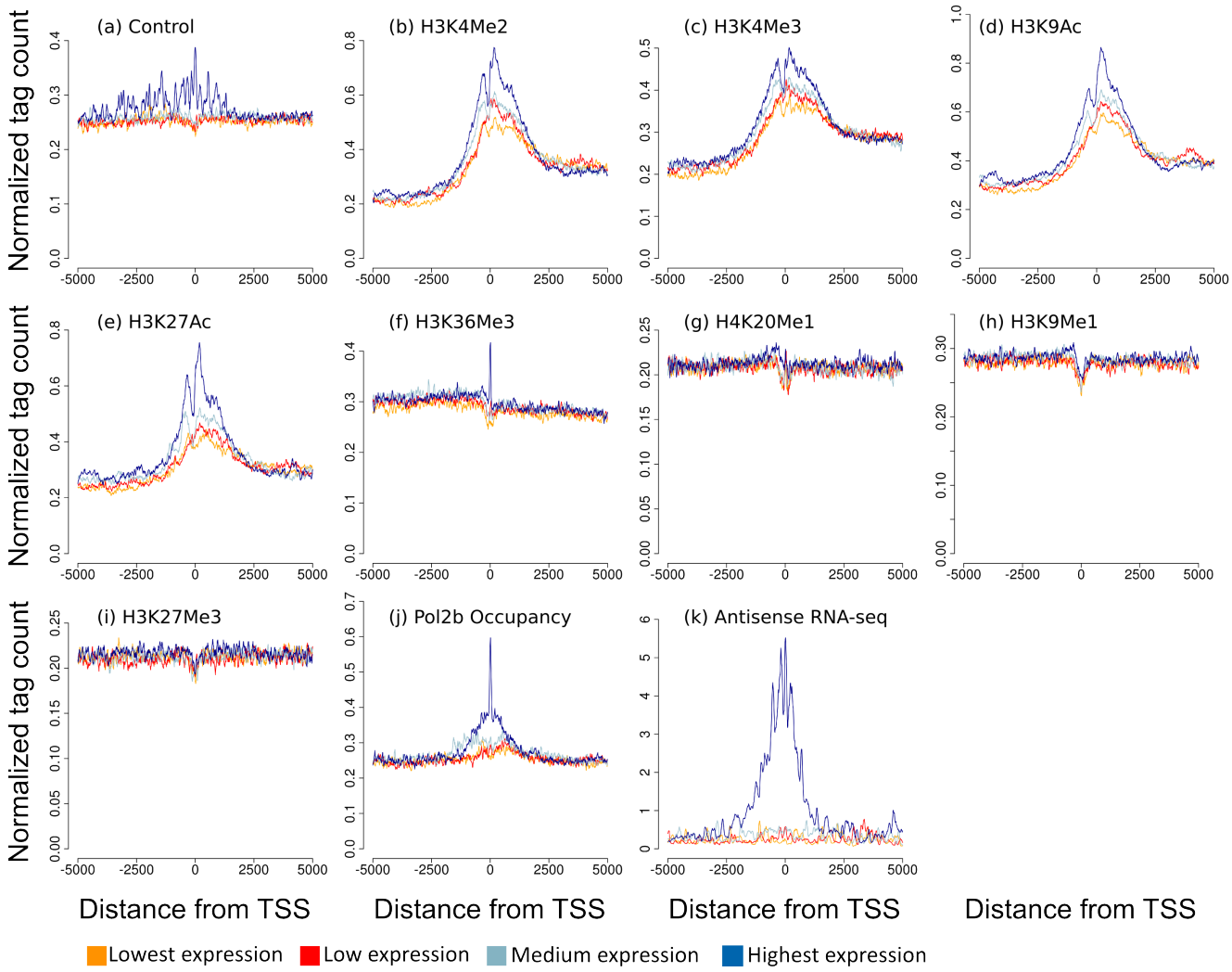

Supplementary Figure S41. Chromatin modification environment around cis-NAT promoters in K562. Cis-NAT promoters in the K562 cell type were identified using CAGE data from polyadenylated RNA from cytosol isolates. Cis-NAT promoters were divided into 4 bins based on their activity (lowest to highest), and the normalized average numbers of ChIP-seq reads in 10 base-pair windows +/- 5kb of the cis-NAT TSS (at position 0) were calculated for each bin.

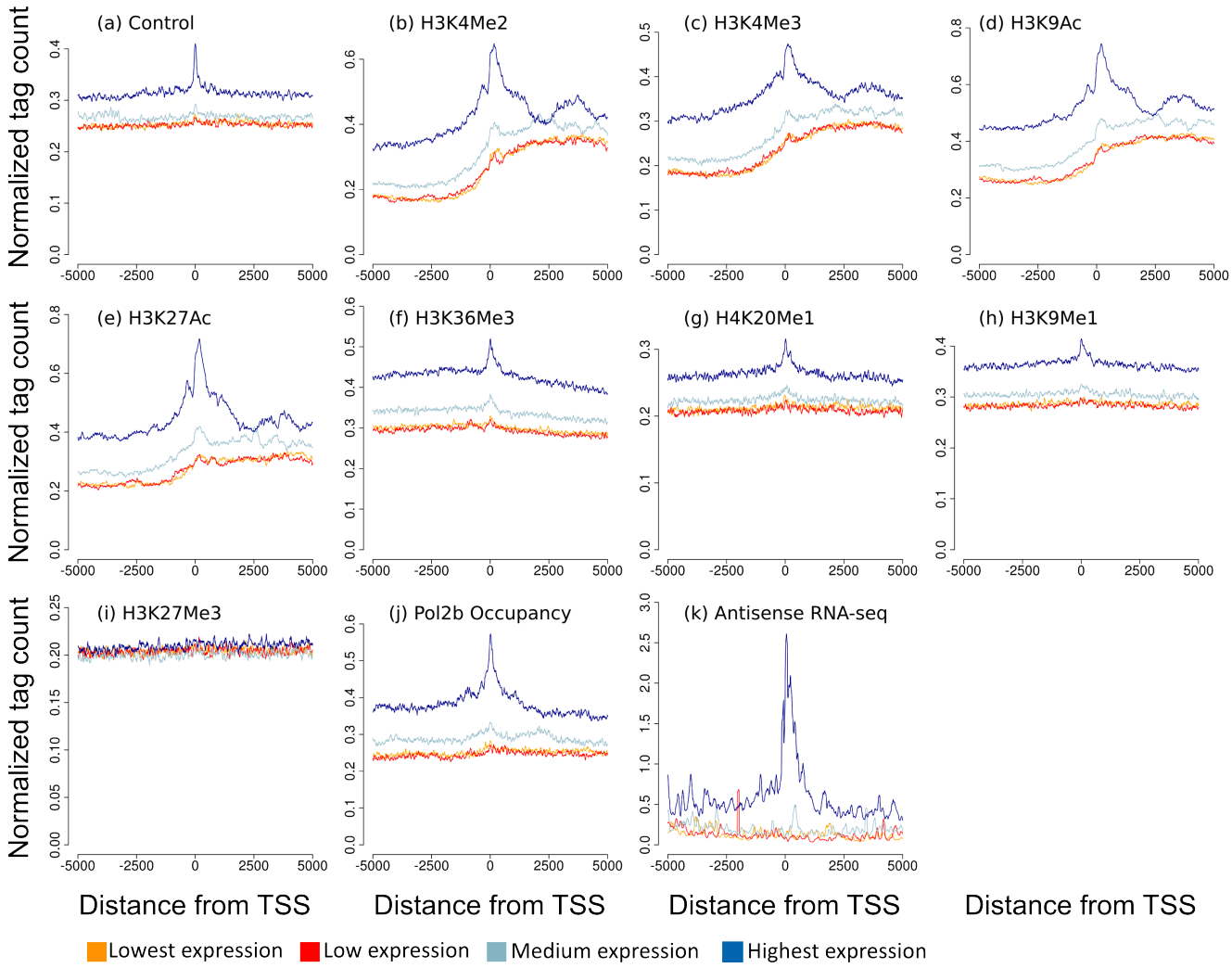

Supplementary Figure S42. Chromatin modification environment around cis-NAT promoters in K562. Cis-NAT promoters in the K562 cell type were identified using CAGE data from total RNA from nucleolus isolates. Cis-NAT promoters were divided into 4 bins based on their activity (lowest to highest), and the normalized average numbers of ChIP-seq reads in 10 base-pair windows +/- 5kb of the cis-NAT TSS (at position 0) were calculated for each bin.

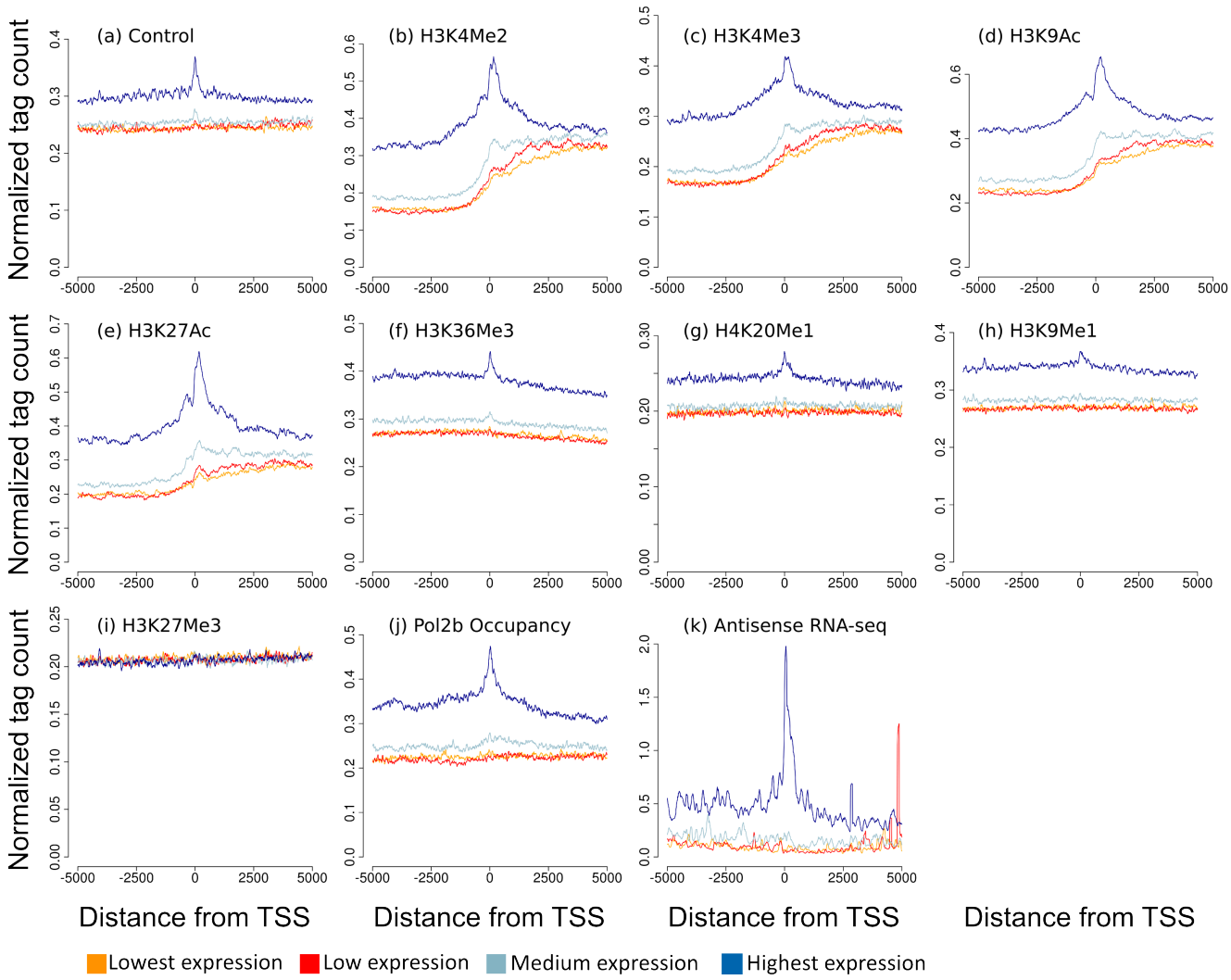

Supplementary Figure S43. Chromatin modification environment around cis-NAT promoters in K562. Cis-NAT promoters in the K562 cell type were identified using CAGE data from total RNA from nucleoplasm isolates. Cis-NAT promoters were divided into 4 bins based on their activity (lowest to highest), and the normalized average numbers of ChIP-seq reads in 10 base-pair windows +/- 5kb of the cis-NAT TSS (at position 0) were calculated for each bin.

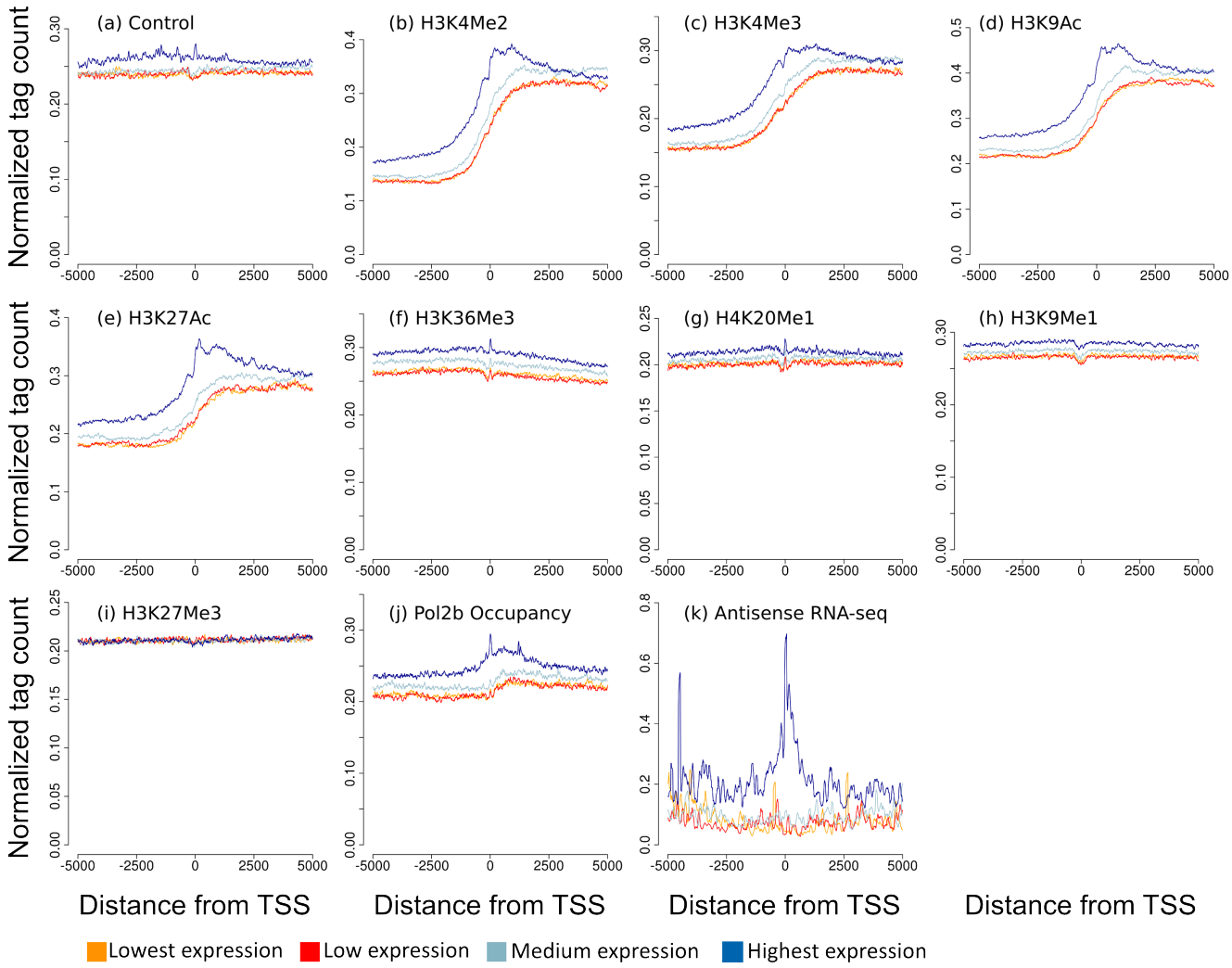

Supplementary Figure S44. Chromatin modification environment around cis-NAT promoters in K562. Cis-NAT promoters in the K562 cell type were identified using CAGE data from non-polyadenylated RNA from nucleus isolates. Cis-NAT promoters were divided into 4 bins based on their activity (lowest to highest), and the normalized average numbers of ChIP-seq reads in 10 base-pair windows +/- 5kb of the cis-NAT TSS (at position 0) were calculated for each bin.

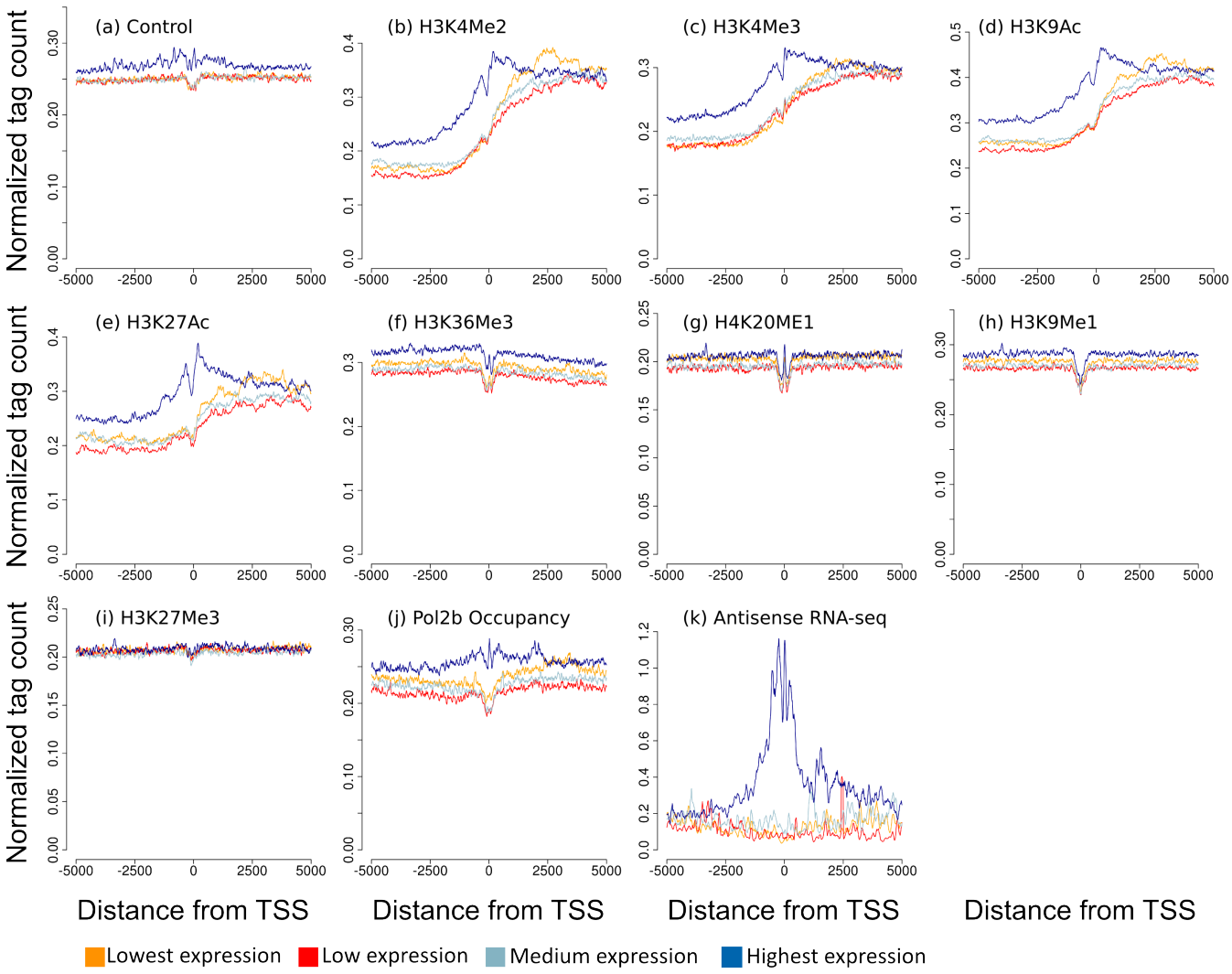

Supplementary Figure S45. Chromatin modification environment around cis-NAT promoters in K562. Cis-NAT promoters in the K562 cell type were identified using CAGE data from polyadenylated RNA from nucleus isolates. Cis-NAT promoters were divided into 4 bins based on their activity (lowest to highest), and the normalized average numbers of ChIP-seq reads in 10 base-pair windows +/- 5kb of the cis-NAT TSS (at position 0) were calculated for each bin.

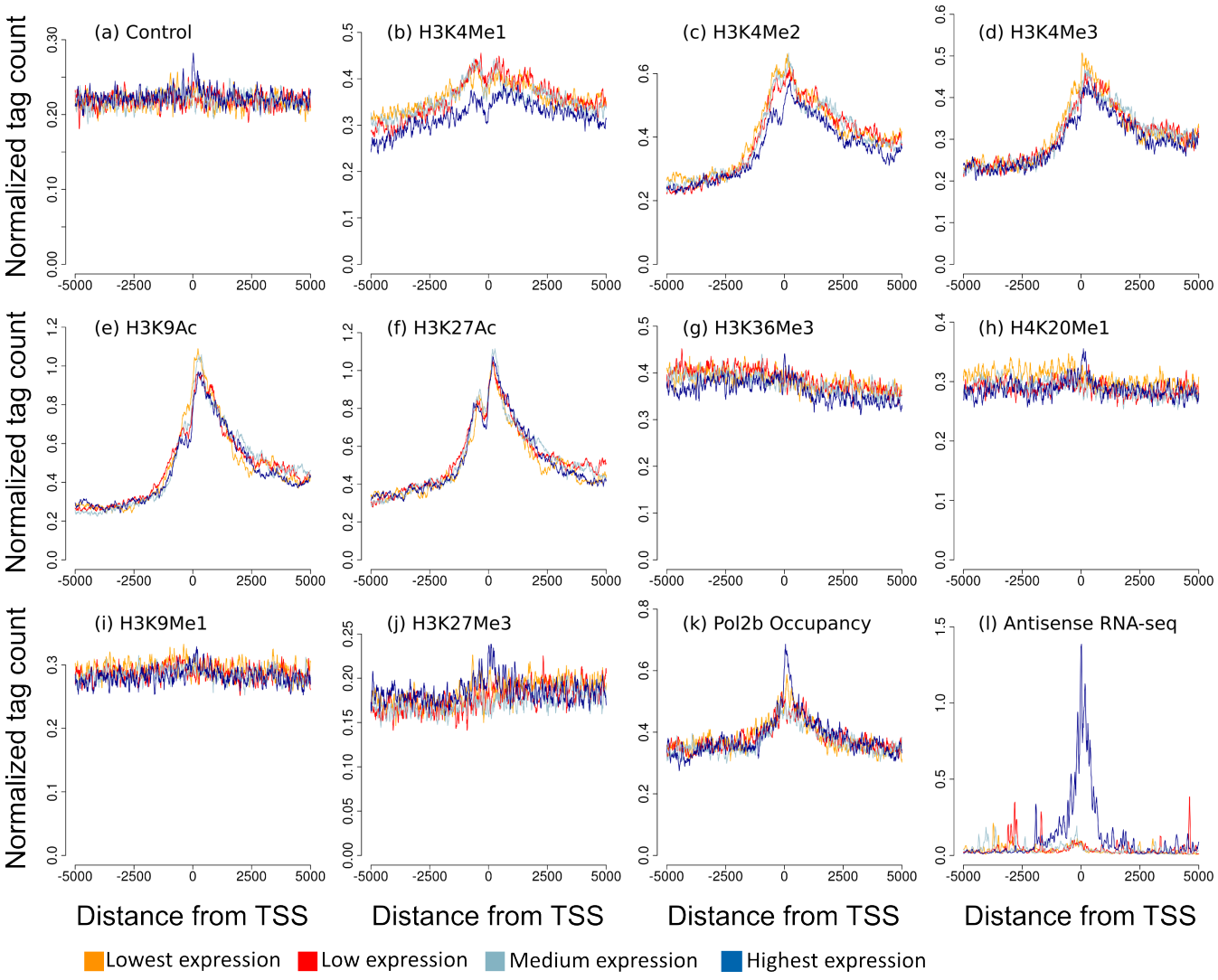

Supplementary Figure S46. Chromatin modification environment around cis-NAT promoters in NHEK. Cis-NAT promoters in the NHEK cell type were identified using CAGE data from non-polyadenylated RNA from cytosol isolates. Cis-NAT promoters were divided into 4 bins based on their activity (lowest to highest), and the normalized average numbers of ChIP-seq reads in 10 base-pair windows +/- 5kb of the cis-NAT TSS (at position 0) were calculated for each bin.